https://doi.org/10.5194/egusphere-2026-4058
Preprint. Discussion started: 20 August 2026

The thermal regime of the Whymper hanging glacier under climate change (Grandes Jorasses, 4050 m a.s.l., Italy)

Adrien Gilbert[1], Fabrizio Troilo[2], Olivier Gagliardini[1], Christian Vincent[1], Paolo Perret[2,3], Luca Mondardini[2], Luc Piard[1], Olivier Laarman[1], and Emmanuel Le Meur[1]

[1]Univ. Grenoble Alpes, CNRS, IRD, Grenoble INP, INRAE, IGE, 38000 Grenoble, France
[2]Fondazione Montagna Sicura - Montagne sûre, Courmayeur, 11013, Italy
[3]Dept. of Electrical, Computer Science and Biomedical Engineering, University of Pavia, Via Ferrata 1, 27100 Pavia, Italy

Correspondence: Adrien Gilbert (adrien.gilbert@univ-grenoble-alpes.fr)

Abstract.

Glaciers in the European Alps are typically cold above 3500–3800 m a.s.l., which allows the formation of steep hanging glaciers. Rising air temperatures and increased surface melting are now altering their thermal regime, raising questions about when and where their bases will start to thaw which could potentially cause them to destabilize. In this study, we report unique observations of long-term temperature change (1997–2021) on the Whymper hanging glacier (4050 m a.s.l.) located on the southern side of the Grandes Jorasses (Italy). Using a state-of-the-art thermo-mechanical model and heat-flux calculations for the entire Grandes Jorasses range, we find that the observed significant temperature changes are driven by rapid surface warming since the 1990s, due to enhanced melting which has ultimately produced persistent temperate surface conditions over the past decade. Remarkably, we demonstrate that the cold basal condition will persist for several years sustained by strong negative heat flux from the colder north face of the Grandes Jorasses, though it may approach melting point temperature by 2050. However, this evolution depends on the amount of water that will percolate through ice fractures at depth, a poorly understood process that could accelerate warming. This underscores the need for continued ice-temperature monitoring in the future.

1 Introduction

Climate change is causing mountain glaciers to evolve into a new state. This transitional phase is characterised by changes in glacier geometry, surface melt-rate and internal temperature, which occur at different timescales. This phase is prone to glacier instability when the balance of forces within a given ice mass is disrupted by a change in its internal or basal conditions. This is typically the case for high-altitude, cold hanging glaciers, for which the surface balance is not significantly affected by climate change (Vincent et al., 2007a, 2020), whereas the internal temperature can change drastically (Gilbert and Vincent, 2013; Hoelzle et al., 2011; Mattea et al., 2021). In particular, the transition from a cold to a temperate base significantly alters the frictional conditions and can result in an imbalance of forces and the collapse of large ice masses (Pralong and Funk, 2006; Faillettaz et al., 2015).

https://doi.org/10.5194/egusphere-2026-4058
Preprint. Discussion started: 20 August 2026

It is important to estimate from when cold glaciers may start to thaw at their base and become unstable, as this would greatly help with managing glacier hazards in potentially affected populated areas. This requires both the observation and modelling of the internal temperature response of glaciers to climate variations, which is not an easy task, given the difficulty of accessing the inner ice of such glaciers and the complexity of the processes affecting their temperature. The glacier temperature field is indeed the result of a combination of energy transport through advection/diffusion (Blatter and Hutter, 1991; Aschwanden et al., 2012) and energy production from strain heating (Cuffey and Paterson, 2010) and latent heat potentially released by water percolation (Phillips et al., 2010; Gilbert et al., 2020). Near-surface temperatures below the active layer through which the climate drives the inner temperature also depend on numerous factors, such as the thickness and density of snow/firn, skin surface temperature, and meltwater percolation and refreezing in the snow/firn (Sauter et al., 2020). Moreover, the temperature field is affected by heat flux from the ground, which can be challenging to calculate in a mountainous area (Noetzli et al., 2007).

Providing an estimation of past and future thermal change thus requires a complete thermo-mechanical modeling of glacier evolution with a good representation of the energy exchanges at the different boundary interfaces with atmosphere and rock substratum. Such modeling approach in a mountain environment was originally initiated by Lüthi and Funk (2001) in two dimensions at Col Gnifetti (Monte Rosa, Switzerland) and by Zwinger et al. (2007) in three dimensions, but only in a steady-state condition and with a specific geometry associated with an ice-filled volcanic crater in Kamchatka (Russia). This was later improved upon by using the enthalpy as the internal energy variable (Gilbert et al., 2014a) and including a more physical approach to compute the surface boundary conditions (Gilbert et al., 2014b). This later model was used to simulate the three-dimensional temperature evolution of the Col du Dôme glacier in the Mont Blanc range (France) from 1907 to 2100, with a full coupling of the density, velocity and temperature fields (Gilbert et al., 2014a). This approach has since been used to simulate the temperature evolution of the Taconnaz hanging glacier in the Mont Blanc range (Gilbert et al., 2015) and to assist the interpretation of ice cores at Colle Gnifetti, Swiss/Italian Alps (Licciulli et al., 2020). Gilbert et al. (2015) demonstrate that the model performs well in reproducing temperature observations, and that large areas may reach the melting point by the end of the 21st century. However, as the thermal regime is determined by numerous factors, each glacier requires a dedicated analysis to assess its precise past and future changes.

This study focuses on the Whymper serac, which is located on the south face of the Grandes Jorasses in the Mont Blanc range in Italy, at an altitude of around 4,050 metres above sea level (a.s.l.) (see Faillettaz et al. (2016); Dematteis et al. (2021) for a general overview). It is a steep hanging glacier frozen to its bedrock which regularly generates ice avalanches following the collapsing cycle of the seracs. In winter, when combined with snow, the ice avalanche can reach the valley and pose a threat to the population and infrastructure of Val Ferret (Margreth et al., 2011; Perret et al., 2021). The glacier has therefore been intensively monitored for many years, with continuous recording of the surface flow velocity, which can indicate whether a major destabilization is about to occur (Faillettaz et al., 2016; Dematteis et al., 2021; Margreth et al., 2011; Perret et al., 2021). Like all cold hanging glaciers, the evolution of the thermal regime of this glacier is of concern, as a very large destabilization could occur if the base of the glacier reaches the melting point. Its thermal regime has been first observed in 1997 (Pralong and Funk, 2006) showing heterogeneous but cold basal condition. It is known that cold glaciers in the Mont Blanc range

https://doi.org/10.5194/egusphere-2026-4058
Preprint. Discussion started: 20 August 2026

have warmed significantly in recent decades (Vincent et al., 2007b; Gilbert and Vincent, 2013; Gilbert et al., 2015) and this is likely to be the case for the Whymper serac. The present study quantifies the ongoing warming by presenting new borehole observations conducted in 2021 and by estimating the past and future temperature evolution of the Whymper Glacier through thermo-mechanical modelling of ice and firn. First, the model is validated by comparing the historical simulations with borehole observations from 1997 and 2021. The calibrated model is then forced using future climate scenarios to estimate the period during which the glacier may unfreeze from its bed and become potentially unstable. Several hypotheses regarding deep water percolation and the influence of heat flux within the Grandes Jorasses massif are analyzed.

2 Data and Method

2.1 Temperature observations

The thermal regime of Whymper Serac has been monitored by borehole temperature measurements during two different field campaigns in 1997 by ETH (Zurich) (Pralong and Funk, 2006) and in 2021/2022 by IGE (Grenoble) (Figure 1). These observations reveal cold-based conditions that are still present in 2021, despite the overall warming of the glacier (Figure 1e-1h). Both campaigns also revealed strong spatial variability over short distances, showing that measurements may be affected by local effects, such as air circulation and/or deep water percolation within existing crevasses. Nevertheless, the presence of a temperate borehole in 2021 (Figure 1d, site 1 in red) may indicate the existence of an unfrozen part of the glacier that could extend towards its western side where temperatures are unknown. This borehole also corresponds to the warmer temperature measured in 1997 (Figure 1c) even though the locations are not exactly the same. Dates, coordinates and depth of the different boreholes are provided in Table 1.

To constrain heat fluxes within the Grandes Jorasses (see section 2.5) we also used 6-years timeseries of ground temperature measured at 55 cm-depth by three sensors installed in 2009 at about 4050 m a.s.l. around the Whymper Glacier (two on the south side and one on the north side; see the blue diamonds in Figure 1a).

2.2 Topography and surface velocities observations

The surface velocities of the Whymper Glacier have been recorded at various times between 2010 and 2021 using a Robotic Total Station to monitor prism positions, or via continuous in-situ GNSS records (Dematteis et al., 2021; Faillettaz et al., 2016). In addition, the surface topography is available thanks to multiple digital elevation model (DEM) acquisitions via satellite (PLEIADES in 2020 and 2021) and drone imagery (2021). Ground-penetrating radar measurements were performed in 2010, enabling the bedrock topography to be reconstructed.

2.3 Meteorological data

Daily temperature and precipitation that are needed to force the model are taken from the SAFRAN reanalysis (Vernay et al., 2021) given for the Mont Blanc range at 4200 m a.s.l. and for the period 1958-2023. These data have been extended to cover

https://doi.org/10.5194/egusphere-2026-4058
Preprint. Discussion started: 20 August 2026

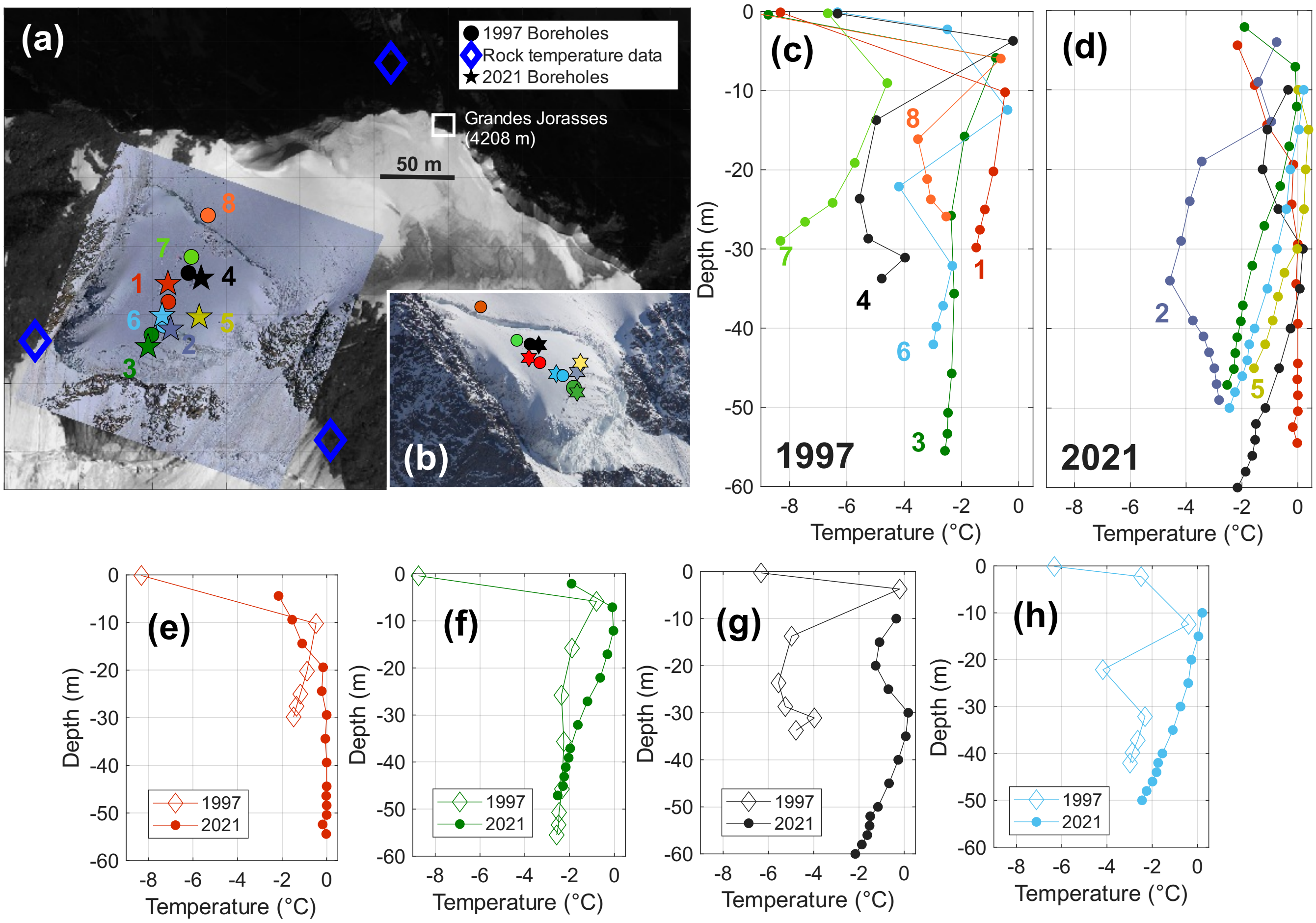

Figure 1. (a) Map of Whymper serac with boreholes location in 1997 (dots) and 2021 (stars). (b) Drone picture from November 2021 with the approximate location of the different boreholes. (c) Temperature measurement from 1997. (d) Temperature measurement from 2021. (e-h) Comparison between observed temperature profile in 1997 and 2021 at boreholes 1, 3, 4 and 6.

the period back to 1907 using temperature and precipitation records from the Lyon-Bron and Besse-en-Oisans meteorological stations (France), respectively. The stations data are corrected, to be consistent with the SAFRAN reanalysis, using quantile-quantile mapping methods, as described in Clauzel et al. (2023). The air temperature values are then corrected for the elevation of a given surface node using a constant lapse rate set to 0.0058 K m^{-1}. Given the uncertainty on snow accumulation at the Whymper Glacier, the precipitation is taken as spatially constant over the model domain, and is corrected so that the modeled steady-state ice flux matches the observations (see section 3.2). The future climate scenarios are taken from the EuroCordex project (Jacob et al., 2014), which provides local future projections using regional climate models (RCMs) forced by different global climate models (GCMs). Fourteen combinations of GCM/RCM are used for each greenhouse gas emission scenario

https://doi.org/10.5194/egusphere-2026-4058
Preprint. Discussion started: 20 August 2026

Table 1. List of boreholes of the Whymper serac with site number, date of temperature measurement, coordinate of the drilling sites and maximum depth reached. The coordinates of the 1997 boreholes are not known from geodetic measurements, we provide here an estimate of it

Site Number	Date	X (UTM 32)	Y (UTM 32)	Depth (m)
1	1997	343645	5081285	55.5
1	30/09/2021	343656.5	5081322.9	61.8
2	30/09/2021	343658.4	5081289.7	58.0
3	1997	343653	5081292	42.0
3	29/11/2020	343643.1	5081276.8	47.1
4	1997	343656	5081309	30.0
4	27/01/2022	343678.9	5081326.9	60.0
5	27/01/2022	343677.7	5081298.5	50.0
6	1997	343670	5081330	33.6
6	27/01/2022	343652.6	5081299.5	45.0
7	1997	343672	5081342	29.0
8	1997	343683	5081372	26.0

(RCP2.6, RCP4.5 and RCP8.5). All scenarios are corrected to be consistent with the historical temperature and precipitation forcing, using the same method employed for the historical period (Clauzel et al., 2023).

2.4 Glacier thermomechanical model

The thermomechanical model used in this study to simulate past and future temperature changes of the Whymper Glacier mainly follows Gilbert et al. (2014a, 2015) and is solved using the finite element solver Elmer/Ice (Gagliardini et al., 2013) based on the Elmer open-source multi-physics package (http://www.elmerfem.org). The model solves, in a coupled way, the Stokes equation adapted to firn rheology (Gagliardini and Meyssonnier, 1997), the density, the enthalpy and the ice damage (see diagram in Figure 2 and model variables in Table 2). The model is forced by a one-dimensional sub-grid module that computes the surface boundary conditions for enthalpy and surface mass balance (Figure 2).

2.4.1 Model description

Both field and constitutive equations of the model are those presented in Gilbert et al. (2014a) with four main differences:

– We implemented Continuous Damage Mechanics as presented in Gilbert et al. (2015) but with a new advection scheme using a semi-lagrangian approach to transport the damage field (Mosbeux et al., 2025).

https://doi.org/10.5194/egusphere-2026-4058
Preprint. Discussion started: 20 August 2026

- The surface boundary condition is provided as Dirichlet conditions for enthalpy which is computed using a sub-grid, one-dimensional model that solves for heat transport and water percolation/refreezing along a vertical profile at each surface node of the 3D model (see Figure 2). This approach has been previously described in Gilbert et al. (2020).

- Water percolation is simply modeled using a "bucket" approach (Vionnet et al., 2012) where all liquid water refreeze in the first cold layer until it reaches melting point and saturation before accessing to the subsequent layer. Percolation is allowed in firn for density below 800 kg m^{-3} (Verjans et al., 2019), but also above if the extensive principal stress exceed the stress threshold for damage production (Gilbert et al., 2020). This aims to model water percolation through crevasses that open where this criteria is reached.

- The Surface Mass Balance (SMB) is computed following the approach described in Gilbert et al. (2023). In particular, the melt model follows Oerlemans (2001) where the available energy for melting is estimated from the sum of a term proportional to net shortwave radiation and a term proportional to air temperature.

The model is solved using different timesteps, dt_T for the thermal part (enthalpy and water percolation) and dt_M for the mechanical part (Stokes, free surface, mass conservation and damage), as shown in Figure 2. Since the timesteps are set to $dt_T = 1/30$ and $dt_M = 1/10$ of a year, respectively, the different variables evolve very little, so no steady iterations are performed within the timesteps (explicit method). The mechanical and thermal parts of the model are both forced by the sub-grid model, which provides SMB, enthalpy and water input at the corresponding timestep. Following (Gilbert et al., 2020), water percolation is allowed over the whole ice column if ice damage production $f(B,\chi)$ is positive at the surface.

The sub-grid model runs at a daily timestep during dt_T and solves a one-dimensional (1D) heat transport problem, which is forced by surface temperature and melt input, computed by the SMB model (see Figure 2). The vertical resolution is set 0.06 m for a total covered depth of 18m. The modeled average temperature and total water flux at a given depth, $z_{Dir} = 2\sqrt{\frac{k}{c_p \rho} dt_T} \approx 1.5$ m (the characteristic length of thermal diffusion), are extracted and used as the boundary conditions for the enthalpy equation and the water percolation solver, respectively. Each time the sub-grid model is executed, the initial temperature profile and vertical emergence/subsidence velocities are extracted from the 3D model. For the steady-state simulation, the subgrid model runs over a 30-year period with $z_{Dir} = 18$ m to extract the average conditions below the active layer, which are provided to the 3D model.

2.4.2 Model setup for the Whymper Glacier

The mesh is unstructured in the horizontal plane and consist of 6-node prism-type elements for a horizontal resolution of 7 to 20 m and includes the Whymper serac (in red on Figure 3) as well as the upstream area feeding the serac (in blue on Figure 3). The mesh is vertically extruded but refined at the surface down to 1 m for a better resolution of the heat transfers and at the ice/rock interface to better capture the heat production due to strain heating close to the base. The mesh includes a 30m-layer of rock (granite) below the glacier (see brown color in Figure 3) where only thermal diffusion is resolved. The thermal properties of the rock are those of granite. The initial geometry is defined from measurements of the bedrock topography made from

https://doi.org/10.5194/egusphere-2026-4058
Preprint. Discussion started: 20 August 2026

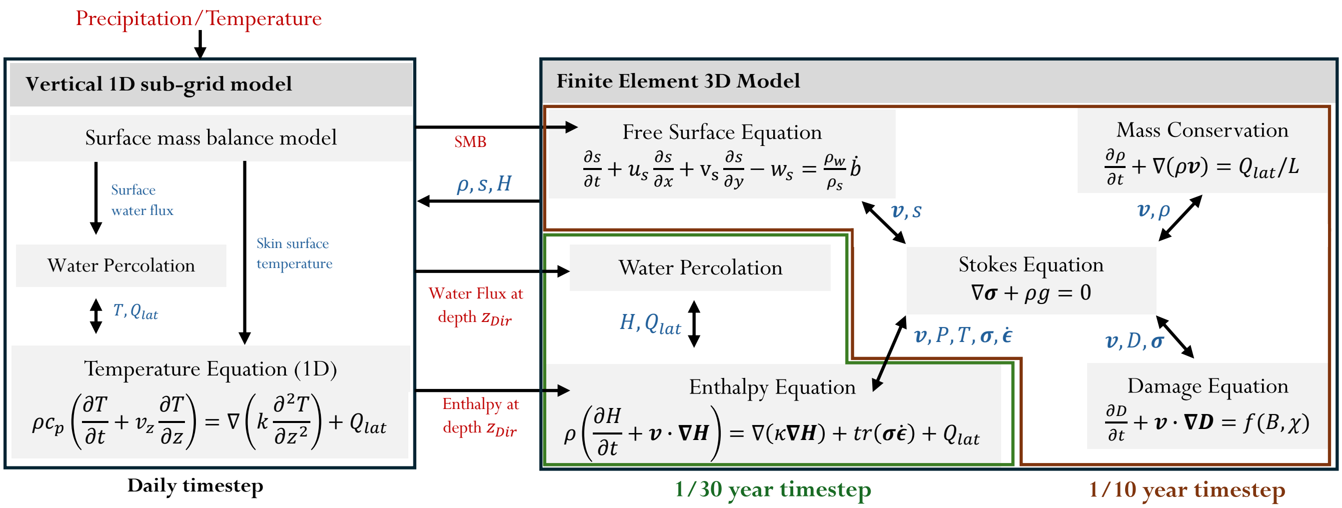

Figure 2. Diagram showing the different equations that are solved and their interactions within the model. Meteorological forcing is provided to the sub-grid model at a daily timestep, which calculates the average enthalpy and total water flux at a given depth z_{Dir} during the 3D thermal simulation timestep (1/30 year). These values are used as a Dirichlet condition for the enthalpy equation and as a source of water input for the percolation solver. Both conditions are provided at depth z_{Dir} in the 3D model. The average SMB during the timestep for the mechanical part (1/10 year) is provided to solve the free surface equation. Definitions of all variables and parameters are given in Gilbert et al. (2014a) and Gilbert et al. (2015).

Table 2. Model variables. Corresponding equations are shown in Figure 2.

Name	Symbol	Value	Unit	Description/Comments
Damage	D	-	-	Damage eq.
Density (firn and ice)	ρ	-	kg m^{-3}	Mass conservation eq.
Enthalpy	H	-	J kg^{-1}	Internal energy. Enthalpy eq.
Surface Mass Balance	$\dot{b}$	-	m w.eq. yr^{-1}	Computed by the SMB model
Pressure	P	-	MPa	Ice isotropic pressure. Stokes eq.
Stress tensor	σ	-	MPa	Stokes eq.
Strain rate tensor	$\dot{\epsilon}$	-	yr^{-1}	Stokes eq.
Surface elevation	s	-	m	Free surface eq.
Temperature	T	-	K	Calculated from enthalpy (Aschwanden et al., 2012)
Velocity vector	$\mathbf{v}$	-	m yr^{-1}	Stokes eq.
Water content	ω	-	-	Calculated from enthalpy (Aschwanden et al., 2012)

ground radar measurement and surface topography measured from drone survey in 2021 and extended using the PLEIADES DEM acquired in August 2020.

https://doi.org/10.5194/egusphere-2026-4058
Preprint. Discussion started: 20 August 2026

Table 3. Parameters of the model and their respective values in this study.

Name	Symbol	Value	Unit	Description/Comments
Firn/ice mechanics				
Damage enhancement factor	B	1.0	-	(Krug et al., 2014)
Damage threshold	σ_{th}	0.1	MPa	(Brondex et al., 2026)
Firn rheological law function	a(ρ)	$exp(13.22240 - 15.78652\ \rho/\rho_i)$	-	(Gilbert et al., 2014a)
Firn rheological law function	b(ρ)	$exp(15.09371 - 20.46489\ \rho/\rho_i)$	-	(Gilbert et al., 2014a)
Flow rate factor	A(T)	Arrhenius law	MPa yr^{-1}	(Cuffey and Paterson, 2010)
Flow rate enhancement factor	E	1.3		
Surface firn density	ρ_s	350	kg m^{-3}	
Thermal regime				
Density (rock)	ρ_{rock}	2800.0	kg m^{-3}	Granite
Heat capacity (ice and firn)	c_p	7.253×T+146.3	J K^{-1} kg^{-1}	(Cuffey and Paterson, 2010)
Heat capacity (rock)	$c_{p_{rock}}$	820.0	J K^{-1} kg^{-1}	Granite
Reference temperature	T_0	200.0	K	(Gilbert et al., 2014a)
Residual saturation	S_r	0.005		(Gilbert et al., 2014a)
Thermal conductivity (ice and firn)	k	f(ρ)	J m^{-1} K^{-1} s^{-1}	(Calonne et al., 2019)
Thermal conductivity (rock)	k_{rock}	3.0	J m^{-1} K^{-1} s^{-1}	Granite
Surface mass balance				
Energy balance at 0°C	k_0	-30.0	W m^{-2}	(Gilbert et al., 2023)
Ice albedo	α_i	0.3		(Gilbert et al., 2023)
Melt factor	k_m	3.0	W m^{-2} K^{-1} day^{-1}	(Gilbert et al., 2023)
Precipitation lapse rate	dP_r/dz	0.0	-	(Gilbert et al., 2023)
Precipitation rate	P_r	1.5	m w.eq. yr^{-1}	(Gilbert et al., 2023)
Radiation factor	R	0.7		(Gilbert et al., 2023)
Snow albedo	α_s	0.8		(Gilbert et al., 2023)
Snow/Rain temperature threshold	T_r	1.0	°C	(Gilbert et al., 2023)
Temperature lapse rate	dT/dz	5.8×10^{-3}	K m^{-1}	(Gilbert et al., 2023)
Physical constants				
Clausius-Clapeyron constant	β	9.7456×10^{-8}	K Pa^{-1}	
Enthalpy of fusion	H_f	$H(T_f)$	J kg^{-1}	$T_f = T_{ptr} - \beta(P - P_{ptr})$
Gravity	g	9.81	m s^{-2}	
Ice density	ρ_i	917.0	kg m^{-3}	
Latent heat of fusion	L	3.34×10^5	J kg^{-1}	
Temperature of water triple point	T_{ptr}	273.16	K	
Pressure of water triple point	P_{ptr}	6.11×10^2	Pa	
Water density	ρ_w	1000.0	kg m^{-3}	

https://doi.org/10.5194/egusphere-2026-4058
Preprint. Discussion started: 20 August 2026

Five distinct boundaries are defined in the modeled domain (see numbering in Figure 3): (1) the ice surface; (2) the rock/ice interface; (3) the base of the domain in the rock; (4) the serac cliff; and (5) the lateral boundaries. The different boundary conditions are set by :

1. Stress-free condition for the Stokes equation. Dirichlet conditions for mass conservation ($\rho = \rho_{surf}$) and enthalpy ($H = H_{surf}$). The condition $H = H_{surf}$ is imposed over a depth z_{Dir} with H_{surf} provided by the sub-grid model.
2. No sliding condition for the Stokes equation.
3. Heat flux for the enthalpy. See Section 2.5 for details on how the heat flux is estimated.
4. Stress-free condition for the Stokes equation. A Dirichlet condition is imposed on the enthalpy, setting it to the air temperature.
5. Zero normal-flux for the Stokes equation. Heat flux for the enthalpy in the rock (see Section 2.5) but zero normal-flux in the ice.

The simulation strategy is to produce a steady state under the climatic conditions of the 1907–1937 period, which serve as the initial conditions for a transient historical simulation from 1930 to 2023. The future simulations restart from the historical simulation and run from 2023 to 2050. The parameter calibration is done by comparing observed and modeled ice thickness, surface velocity and borehole temperature in 1997 and 2021. An initial guess is used for computing the first steady state which is then re-run after parameter calibration. All parameter of the model and their associated values are summarized in Table 3.

2.5 Estimating heat flux within the Grandes Jorasses

The Whymper Glacier is located near the summit of the Grandes Jorasses mountain and is likely influenced by significant heat flux between its north and south faces, especially given the steepness of the north side. Therefore, estimating the heat flux at the rock boundary of the model (boundary conditions 3 and 5; see Figure 3) must account for these thermal transfers which are likely cooling the glacier's base. We thus solve for the three-dimensional heat diffusion problem within the Grandes Jorasses range assuming steady state condition to estimate the heat flux within the mountain (Figure 4a). We estimate steady-state surface conditions using an empirical relationship between air temperature and potential solar radiation. This relationship is derived from ground temperature observations at a depth of 50 cm on both sides of the mountain (Figure 1a). Assuming a temperature lapse rate of 0.0058 K m^{-1}, we find that the annual temperature can be approximated by the following relationship (Figure 4b):

$$T_s(z,R) = 0.0058 \times (4010.0 - z) + 0.03848 \times R - 11.86 \quad (1)$$

where T_s is the rock surface temperature (°C), z the surface elevation (m a.s.l.) and R the potential solar radiation (W m^{-2}). The thermal properties of the rock are assumed to be the same as those used in the glacier model and a geothermal basal flux of 85 mW m^{-2} is imposed at the domain base (Maréchal et al., 1999).

https://doi.org/10.5194/egusphere-2026-4058
Preprint. Discussion started: 20 August 2026

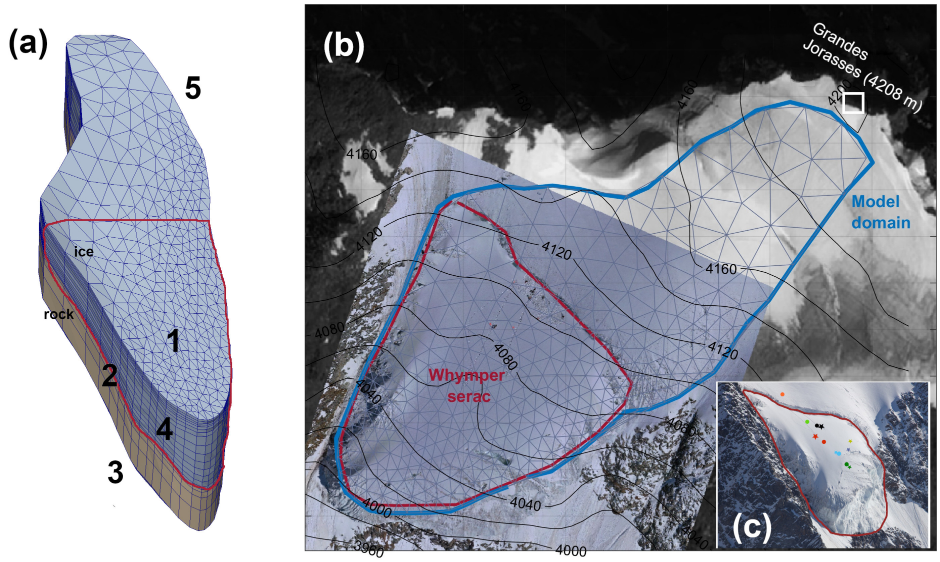

Figure 3. (a) 3D mesh of the glacier including 30 m of rock below the ice. (b) Elevation contours with the model domain shown in blue, along with the associated mesh in light gray. (c) Drone picture of the glacier front. The red line shows the serac contour across the three panels.

3 Modeling results

3.1 Basal heat fluxes

The modeled temperature field within the Grandes Jorasses shows contrasting temperature between the north and south side of the mountain, with frozen condition above 2800 m on the north side and 3700 m on the south side (Figure 4c). It results in a strong heat flux that is almost horizontally going from the south to the north face in the area of the Whymper Serac (Figure 4d-e).

We extract the modeled heat flux component normal to the boundaries 3 and 5 of the glacier model (see Figure 3a) that will be applied as a heat flux boundary condition for the enthalpy equation in the rock. As expected, the normal basal heat flux at the domain base appears to be mainly negative with values ranging from -40 mW m^{-2} to -140 mW m^{-2} close to the summit ridge (Figure 4f). We assume that this flux remains constant through the simulation which is a reasonable assumption given the timescale of temperature change in the rock at this depth (>100 years) .

3.2 Pre-industrial steady state

The "pre-industrial" steady state is obtained by letting the model equilibrate thermally and geometrically in a stationary climate corresponding to the first 30 years of the meterological data (1907-1937). Figure 5 shows the mean surface conditions calculated by the SMB and subgrid model over this period. The stationary surface temperature field varies from approximately 0°C to

https://doi.org/10.5194/egusphere-2026-4058
Preprint. Discussion started: 20 August 2026

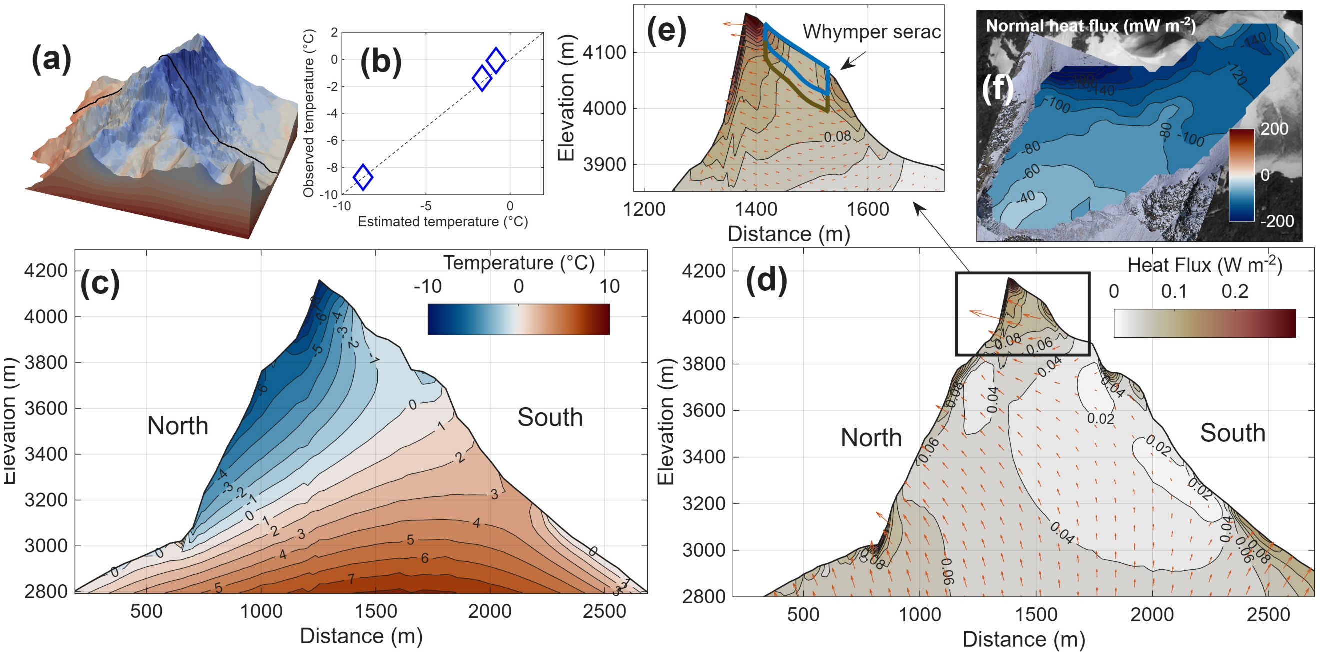

Figure 4. (a) 3D model of the thermal state of the Grandes Jorasses range. (b) Observed and estimated ground temperature at 50 cm-depth (10 years average). (c,d) Modeled steady state temperature (c) and heat flux (d) along the black cross section shown in (a). (e) Zoom on Grandes Jorasses summit. The model domain is shown in blue (ice) and brown (rock). (f) Normal heat-flux (mW m^{-2}) extracted at the base of the domain (boundary 3).

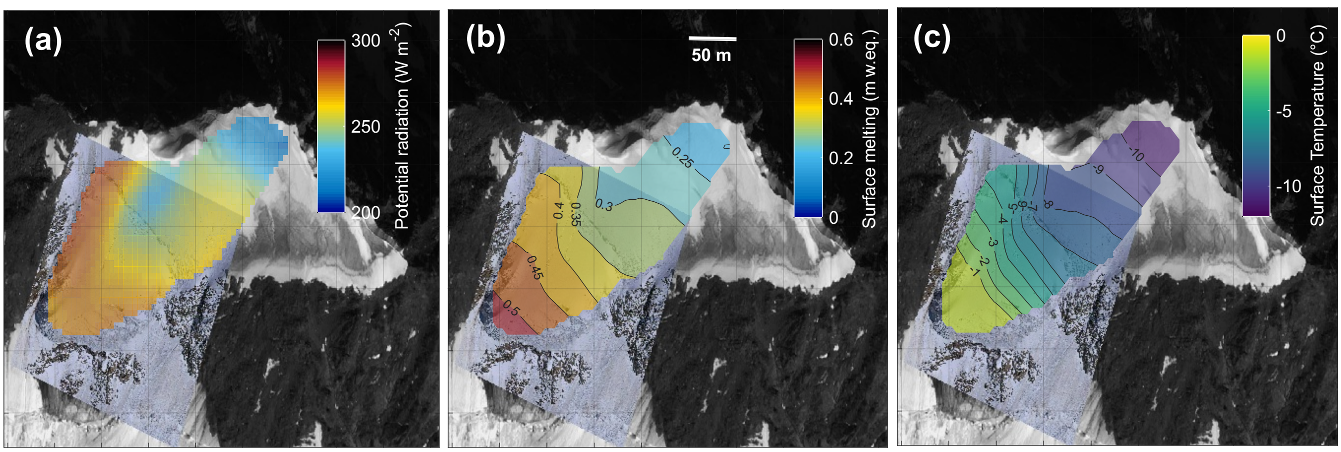

Figure 5. Steady state surface condition at the beginning of the 20^{th} century. (a) Potential solar radiations. (b) Annual surface melting. (c) Near-surface temperature.

https://doi.org/10.5194/egusphere-2026-4058
Preprint. Discussion started: 20 August 2026

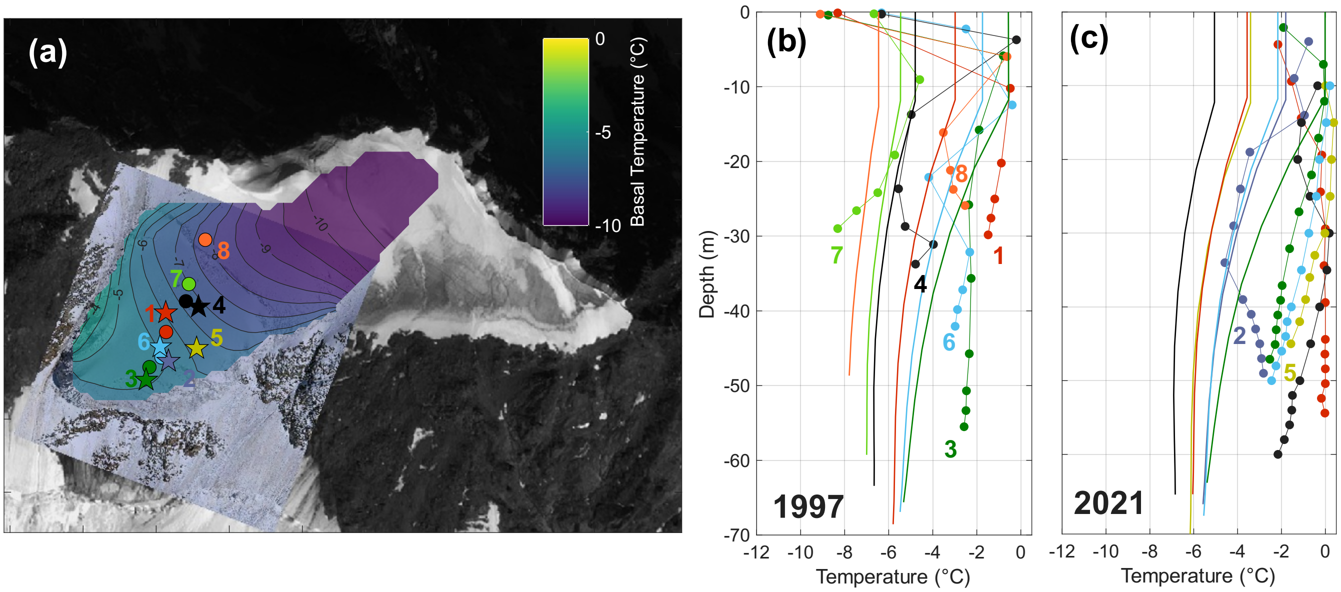

Figure 6. (a) Modeled steady state basal temperature. (b) Modeled steady state temperature (lines) compared to observations in 1997 (dotted lines). (c) Modeled steady state temperature (lines) compared to observations in 2021 (dotted lines). The difference in the simulated temperature profiles (b) and (c) is due to the different borehole locations.

-10°C (Figure 5c) showing a rapid increase in surface temperature with decreasing elevation in response to an increase in melting increase from 0.2 m w.eq. yr^{-1} to 0.5 m w.eq. yr^{-1} (Figure 5b). Melt increase is due to both rising air temperature and potential shortwave radiation at lower elevation (steeper and south-facing slopes close to the serac cliff).

Steady state temperatures are found to be entirely cold with basal temperature comprised between -5°C and -11°C (Figure 6a). The western side of the glacier is found to be warmer due to the influence of stronger incoming solar radiation and thus surface melting (Figure 5), but also because this side of the glacier is less affected by colder ice advection coming from the summit area. The influence of the air-exposed serac boundary is visible and cool down basal temperature of up to 2°C in a small area extending up to about 20 m from the serac influencing borehole sites 2, 3 and 6. Comparison with englacial measurement in 1997 (Figure 6b) shows that temperature at that time were still close to steady condition and that most of the warming happened afterward (Figure 6c).

3.3 Past century evolution

The historical simulation runs from 1930 to 2023 using the steady state simulation as an initial condition. In order to estimate the mean snow accumulation, we performed a grid search on mean snow accumulation and Glen's law flow enhancement factor E (Cuffey and Paterson, 2010) to find the best match with both the observed thickness in 2021 and surface velocities at stakes 4 (July-October 2014) and 13/14 (October 2011 to September 2013) (Dematteis et al., 2021; Faillettaz et al., 2016) (stakes are shown in Figure 7a). We found a unique solution involving a 30% increase in flow rate factor and an average snow

https://doi.org/10.5194/egusphere-2026-4058
Preprint. Discussion started: 20 August 2026

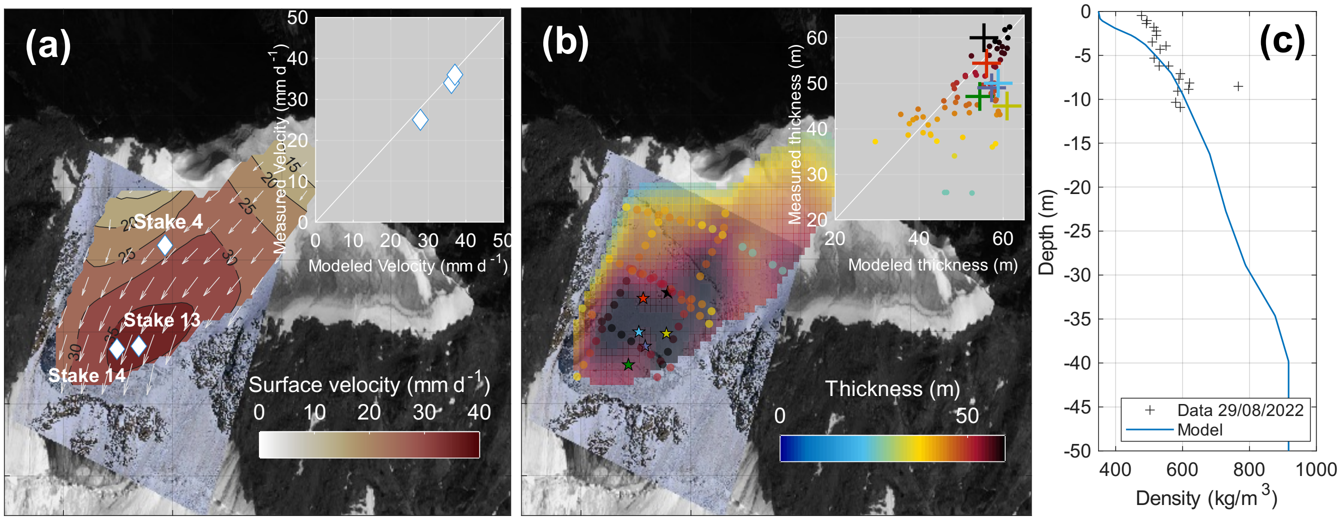

Figure 7. Modeled velocities, thickness and density in 2021. (a) Modeled surface velocity (mm d^{-1}) and location of the monitored stakes for surface displacement (orange dots). The inset shows comparison between modeled thickness and observed thickness. (b) Modeled (colormap) and observed thickness by GPR (dots). The inset shows comparison between modeled thickness and observed thickness. Color dots are GPR measurements and cross are boreholes depth. (c) Modeled and observed density close to the middle rimaye in August 2022.

accumulation of 1.5 m w.eq. yr^{-1} which shows good agreement with both surface velocities (Figure 7a) and thickness (Figure 7b). We note that the original flow rate factor is given by the classical Arrhenius relationship with temperature (Cuffey and Paterson, 2010). The modeled density is also found to agree well with the measured density profile near site 7 in August 2022 (Figure 7c). Given the melt rate, the average surface mass balance is thus estimated at 1.15 m w.eq. yr^{-1} at the beginning of the simulation and decreasing to 0.9 m w.eq. yr^{-1} over the last decade, driving only 5% of thickness change. We note that the steady-state simulation was run again using the correct accumulation, even though it has no influence on the simulated temperatures in 1997 and 2021.

Modeled temperatures show an overall good agreement with temperature observation in 1997 and 2021 (Figure 8). However, each borehole temperature profiles are not necessarily very well captured individually, especially in 1997. It seems that temperature observations are affected by small scale local effect that are not taken into account in the model such as the air circulation in an open crevasse that likely has a cooling effect on site 2 or site 7 (Figure 8). The fact that the site 1 is temperate in 2022 (Figure 8) may not be a local effect as this borehole is the most western temperature measurement where temperature tend to increase according to the model. It would mean that the western side of the glacier may already be entirely temperate.

The most remarkable result is that the surface temperature condition has become entirely temperate over the last six years (since 2016), as modeled in 2022 (see Figure 8e). This finding aligns with the 2021 observations, which revealed temperate conditions in most boreholes at a depth of 20 meters, which is below the active layer (Figure 8f). This suggests that the entire glacier will warm in the coming decades with little sensitivity to future climate change, as the 0°C threshold has already been reached below the active layer. In this context, the evolution of the basal temperature is primarily controlled by the heat flux

https://doi.org/10.5194/egusphere-2026-4058
Preprint. Discussion started: 20 August 2026

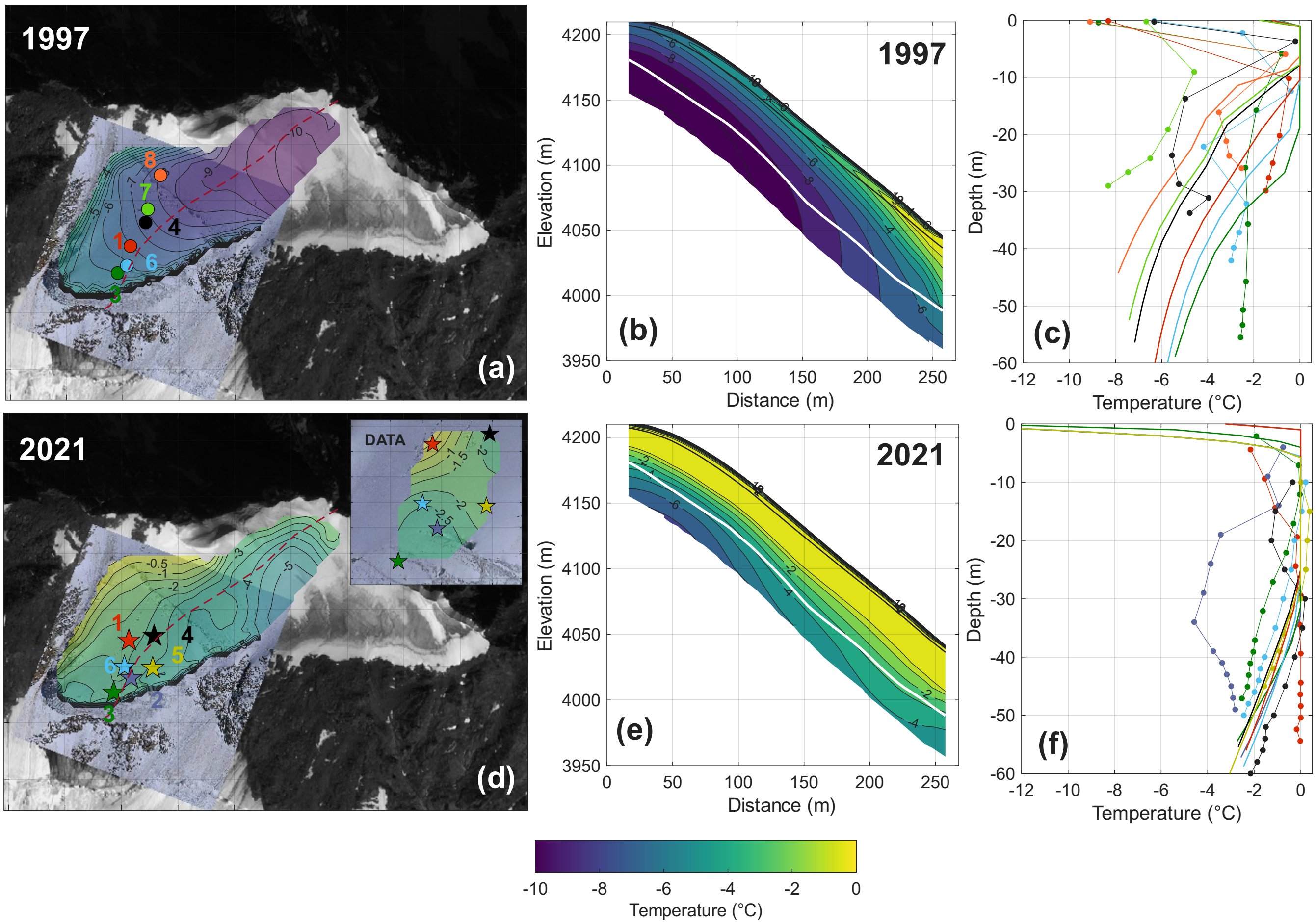

Figure 8. Modeled temperature in 1997 and 2021. (a,b) Basal temperature. (c,d) Temperature along the red dashed line shown in (a) and (b). The white bold line is the ice-rock interface. (e,f) Comparison between model (lines) and observations (dots) at the different boreholes.

within the Grandes Jorasses and the amount of water that percolates through the ice along fractures. Competition between these two phenomena will determine whether the glacier base will thaw in the coming decades.

3.4 Future evolution

We present here the averaged englacial temperature obtained from all GCM/RCM output forced by the scenario RCP4.5. The results obtained with the other RCP scenarios are identical as they all impose the same temperate surface condition (at 0°C). We thus do not distinguish the different RCPs in the following. Our simulation shows that a permanent regime is reached by 2050 where the ice temperature equilibrates between surface temperate condition and the heat flux pumping out energy at the glacier boundary. The resulting basal temperature would remain mainly cold even in 2050 although the basal temperatures are modeled to be close to melting point (above -1°C) in large parts of the glacier (Figure 9).

https://doi.org/10.5194/egusphere-2026-4058
Preprint. Discussion started: 20 August 2026

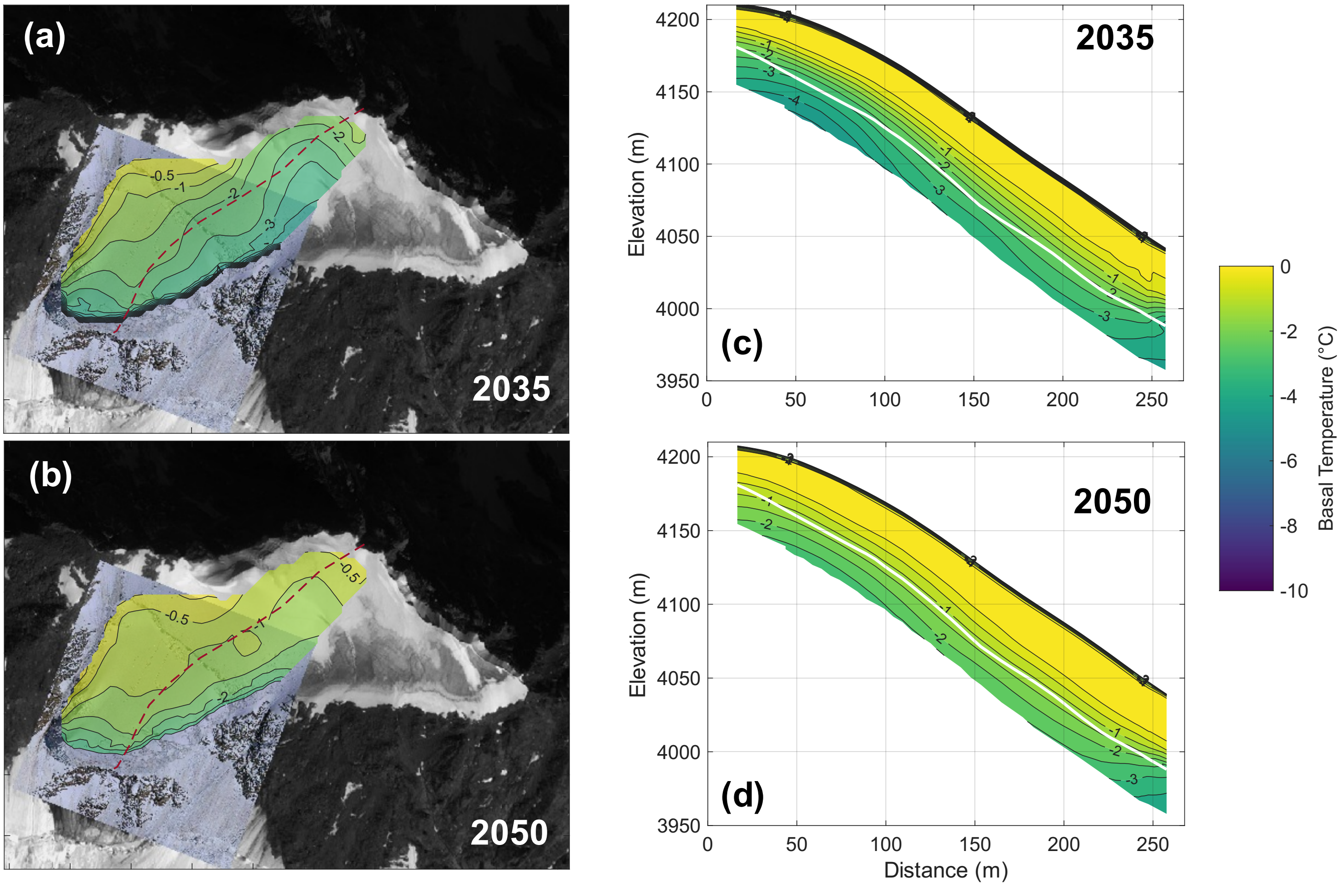

Figure 9. (a,b) Modeled basal temperature in 2030 and 2050. (c,d) Modeled temperature in 2030 and 2050 along the longitudinal section shown in (a,b) (red dashed line). The white bold line is the rock-ice interface.

Thus, the future evolution of the basal temperature of the Whymper serac does not depend on future climate conditions. Unlike in the last few decades, when the surface temperature changed significantly from cold to temperate, the surface temperature is now mainly temperate and will remain so in the future. It will be rather determined by how much water will reach the bedrock and how the heat flux in the rock will evolve in response to the warming of the whole Grandes Jorasses mountain. We note that the modeled average surface mass balance reaches 0.5 m w.eq. yr^{-1} in 2050 due to increasing melt, which leads in a decrease in ice thickness of around 20%, compared to the steady state, and contributes to warmer basal conditions.

4 Discussion

4.1 Role of deep water percolation through cold ice

In the absence of water infiltration within the ice, the basal temperature of the Whymper serac would remain below freezing even under temperate surface conditions, due to the negative temperature gradient imposed by the heat flux towards the cooler north face. In this specific situation, deep water percolation through cold ice plays a critical role in determining the basal temperature of the glacier, as it is the only way to reach basal temperate conditions. Our simulations show that this process may explain about +1°C in the current and future modeled basal temperature (Figure 10) which is not enough to compensate for the basal heat flux and to maintain basal temperate condition.

However, we acknowledge that the extent to which the model captures the effect of deep percolation is highly uncertain, given the discrete nature of crevassing and fracturing, compared to the continuous damage mechanics approach used here to estimate where the crevasses form. Figure 10a shows the depth average damage modeled in 2021 with the red circle showing the main damage production area. This area does correspond to a large crevasse that is often visible (see inset of Figure 10a) but the main crevasse crossing the entire glacier is not captured. Modeling the exact location of crevasses at such small scale is rather challenging and other approach based on observed recurrent crevasses location may be more relevant here even though this is not straightforward neither given the evolving nature of the glacier. The observation of a fully temperate borehole in 2021 (site 1, Figure 1e) suggests that the model may underestimate water percolation. However, without additional observations, it is impossible to determine whether this observation is representative of a large area or a very small one.

4.2 Influence of internal heat flux within the Grandes Jorasses peak

Imposing a negative heat flux at the glacier's base significantly affects the modeled temperature evolution, potentially maintaining cold conditions at the ice/rock interface for several decades even when the surface temperature reaches 0°C. Without this effect, the glacier would reach temperate conditions in a large part of its base by 2050 (Figure 11). In that case, the remaining cold area in 2050 (Figure 11) is mainly associated with the cooling of the air-exposed ice cliff due to negative annual air temperatures.

Although it is a very sensitive aspect of the model results, there is little doubt about the existence of such a flux, given the proximity of the north face, which is about 8°C cooler than the southern side (Figure 4b). Its amplitude is also fairly well constrained thanks to our data on both side of the mountain associated with modeled diffusive heat in real geometry. Some uncertainties may come from the fact that we neglect the transient change of this flux, but it is unlikely to play a significant role within the considered timescale, during which warming has mainly occurred since the 1980s. This study highlights the importance of considering the specific heat flux associated with mountainous terrain when studying hanging glaciers located near ridges.

https://doi.org/10.5194/egusphere-2026-4058
Preprint. Discussion started: 20 August 2026

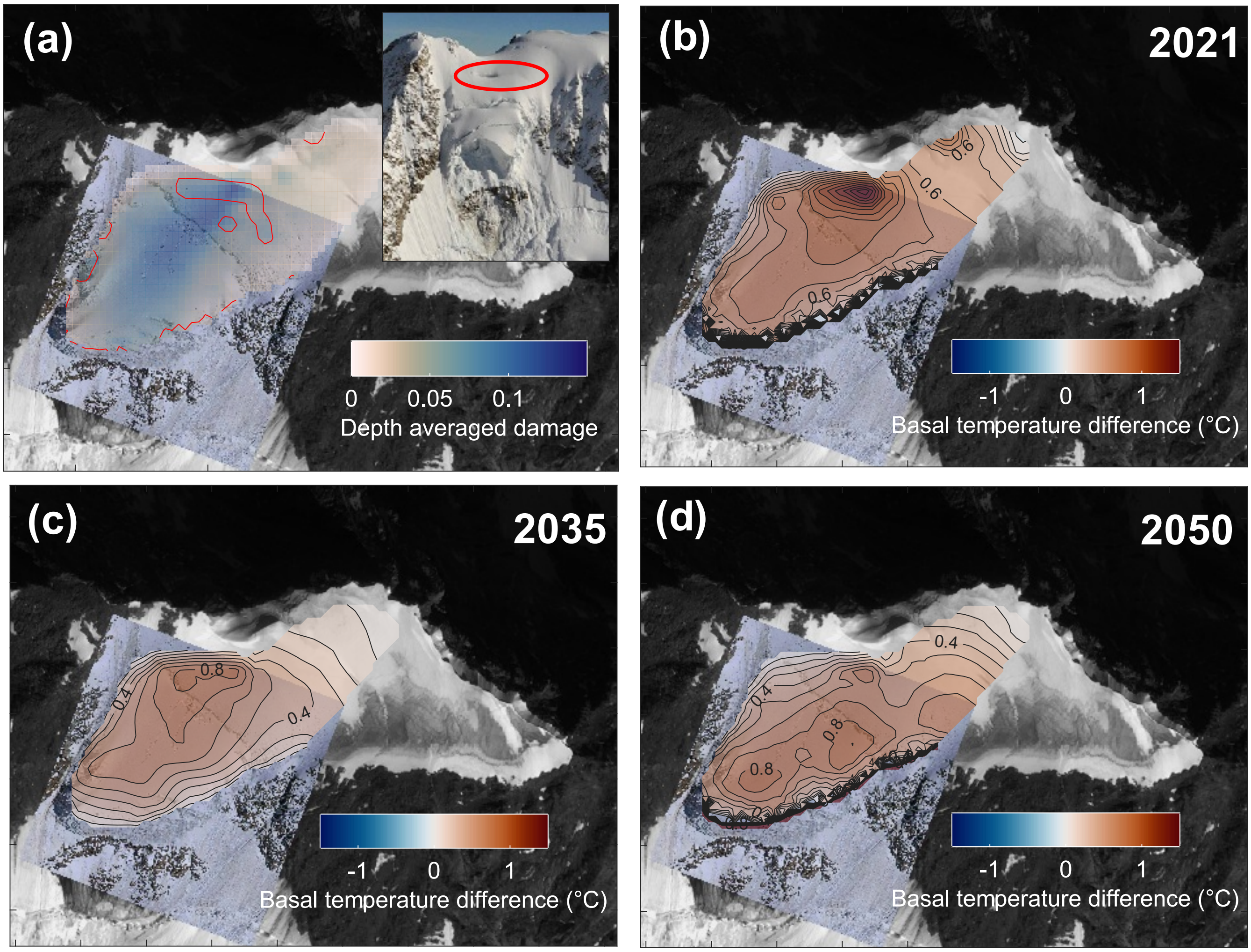

Figure 10. Influence of water percolation through damaged ice. (a) Depth-averaged damage in 2021. The red circle highlights the source of damage ($f(B,\chi) > 0$), which corresponds to a well-marked crevasse that was visible in 2014 (inset picture adapted from Faillettaz et al. (2016)). (b-d) Basal temperature difference between simulation with or without percolation in damaged ice in 2021, 2035 and 2050.

4.3 Implications for the Whymper serac future stability

The primary motivation behind this work is to determine the future stability of the Whymper serac. In this context, it is crucial to identify where and when the ice-rock interface will thaw. As stated in previous sections, the Whymper serac is unique due to its location, which results in a strong negative heat flux that cools the glacier. Without water percolating through the ice, the glacier would actually remain cold and stable in the coming decades. However, it is likely that water percolates, at least locally, thawing some parts of the glacier as shown by the borehole 1 measured in 2021 (Figure 1e).

https://doi.org/10.5194/egusphere-2026-4058
Preprint. Discussion started: 20 August 2026

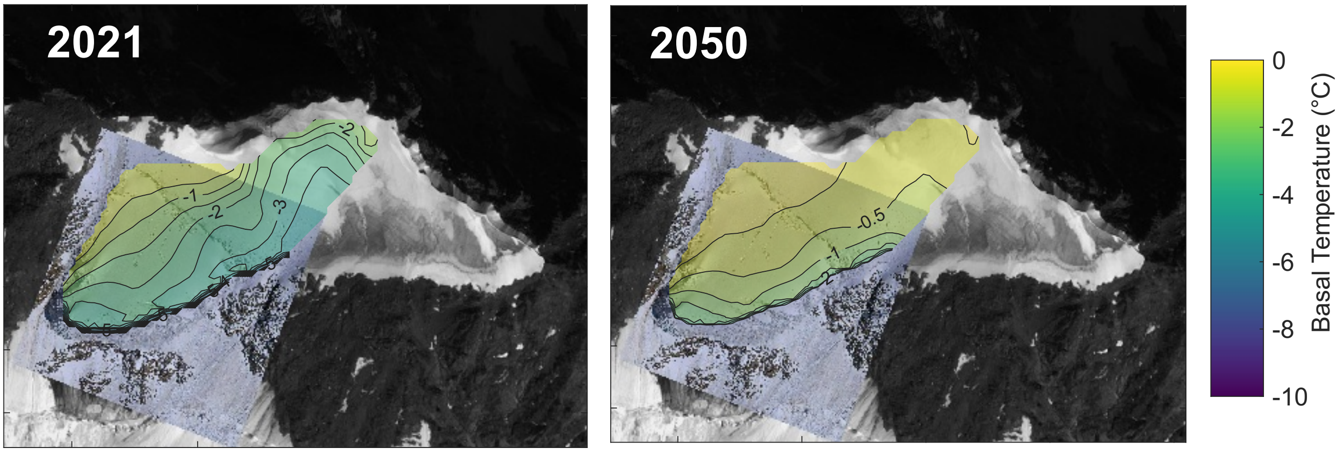

Figure 11. Modeled basal temperature in 2021 and 2050 with the cooling effect from the north face being neglected.

Thus, the future stability of the glacier will be determined by how much meltwater reaches the bed each year and how it spreads at the ice-rock interface. Although there are still large uncertainties regarding how this process is accounted for in the model, our simulation indicates that the western side of the glacier may reach temperatures close to the melting point by 2050, while maintaining cold conditions near the ice cliff (Figure 9). If there is a loss of friction in these warmer parts, the transfer of stress to the frozen front could lead to an unstable situation in which the mechanical resistance of the ice could be exceeded. In this scenario, our simulation indicates a potential volume of collapsed ice of about 500 000 m^3, which would produce a significant ice avalanche impacting the Val Ferret infrastructure (Margreth et al., 2011).

It is also important to note that the Whymper serac will continue to experience partial collapses linked to its "natural" activity, such as the ones that occurred in 1998 and 2014 (Faillettaz et al., 2016). Since surface mass balance is minimally affected by climate change at this elevation, the glacier will always recover from these events. However, this study has not investigated the impact that these events can have on the thermal regime itself. Large collapses from the glacier front entrain a large part of firn layer on the surface, leaving a large scar exposing bare ice (Faillettaz et al., 2016), which would have rather a cooling effect on the glacier (Gilbert et al., 2012).

5 Conclusions

This study reports on and analyzes englacial temperature changes in the Whymper hanging glacier in the Val Ferret region of Italy. Observations show that the glacier is cold-based and experienced significant warming between the 1997 and 2021 drilling campaigns. The measurements also reveal a heterogeneous temperature field, highlighting the local influence of crevasses. These can cool the ice locally by circulating air, or cause deep water to percolate and warm the ice, as demonstrated by significant temperature difference between nearby boreholes. Using three-dimensional thermo-mechanical modeling of the glacier, along with heat flux estimation within the Grandes Jorasses range, we demonstrate that the overall ice warming resulted from a rise in surface temperature, which reached permanent temperate conditions approximately ten years ago (around 2016). However, strong negative heat flux from the north side of the Grandes Jorasses will be able to maintain a cold glacier base, and the future evolution of the basal temperature will depend on the amount of water reaching the bed through ice fractures, a poorly constrained phenomenon. Nevertheless, our results suggest that a significant portion of the glacier will experience temperatures close to the melting point by 2050 while the frontal part will remain cold due to its proximity to the ice cliff, which is in contact with negative atmospheric temperatures. This raises concerns about the glacier's stability in the coming decades and underscores the need for continued close monitoring of this glacier, including detailed surveys of its basal temperature evolution.

Code and data availability. The modeling code is based on the open-source code Elmer/Ice available at http://elmerfem.org/elmerice/wiki/doku.php (last access: 16 June 2026; Elmer/Ice, 2026). The borehole temperature data and the command files to run the simulation are available at https://doi.org/10.5281/zenodo.22014022 (last access: 20 August 2026; Zenodo, 2026).

Author contributions. AG designed and performed the model analysis. AG wrote the manuscript. FT, OG and CV designed and led the field observation campaigns. PP and LM produced velocity data, surface DEMs and bedrock DEM. LP, OL and EL conducted the drilling operation and instrumented the boreholes. All authors contributed to proofreading the manuscript.

Competing interests. The authors declare no competing interest.

Acknowledgements. The study was funded by the Autonomous Region of Valle d'Aosta. We would like to thank everyone involved in the drilling operations and the Environmental Protection Agency of Valle d'Aosta for providing rock temperature measurements. All the computations presented in this paper were performed using the GRICAD infrastructure (https://gricad.univ-grenoble-alpes.fr), which is supported by Grenoble research communities.

https://doi.org/10.5194/egusphere-2026-4058
Preprint. Discussion started: 20 August 2026

References

Aschwanden, A., Bueler, E., Khroulev, C., and Blatter, H.: An enthalpy formulation for glaciers and ice sheets, Journal of Glaciology, 58, 441–457, https://doi.org/10.3189/2012JoG11J088, 2012.

Blatter, H. and Hutter, K.: Polythermal conditions in arctic glaciers, Journal of Glaciology, 37, 261–269, https://doi.org/10.3189/S0022143000007279, 1991.

Brondex, J., Gagliardini, O., Gilbert, A., and Thibert, E.: How to model crevasse initiation? Lessons from the artificial drainage of a water-filled cavity on the Tête Rousse Glacier (Mont Blanc range, France), The Cryosphere, 20, 1655–1677, https://doi.org/10.5194/tc-20-1655-2026, 2026.

Calonne, N., Milliancourt, L., Burr, A., Philip, A., Martin, C. L., Flin, F., and Geindreau, C.: Thermal Conductivity of Snow, Firn, and Porous Ice From 3-D Image-Based Computations, Geophysical Research Letters, 46, 13 079–13 089, https://doi.org/https://doi.org/10.1029/2019GL085228, 2019.

Clauzel, L., Ménégoz, M., Gilbert, A., Gagliardini, O., Six, D., Gastineau, G., and Vincent, C.: Sensitivity of Glaciers in the European Alps to Anthropogenic Atmospheric Forcings: Case Study of the Argentière Glacier, Geophysical Research Letters, 50, e2022GL100 363, https://doi.org/10.1029/2022GL100363, 2023.

Cuffey, K. M. and Paterson, W. S. B.: The physics of glaciers, Academic Press, Amsterdam, 4th ed. edn., 2010.

Dematteis, N., Giordan, D., Troilo, F., Wrzesniak, A., and Godone, D.: Ten-Year Monitoring of the Grandes Jorasses Glaciers Kinematics. Limits, Potentialities, and Possible Applications of Different Monitoring Systems, Remote Sensing, 13, 3005, https://doi.org/10.3390/rs13153005, 2021.

Faillettaz, J., Funk, M., and Vincent, C.: Avalanching glacier instabilities: Review on processes and early warning perspectives, Reviews of Geophysics, 53, 203–224, https://doi.org/10.1002/2014RG000466., 2015.

Faillettaz, J., Funk, M., and Vagliasindi, M.: Time forecast of a break-off event from a hanging glacier, The Cryosphere, 10, 1191–1200, https://doi.org/10.5194/tc-10-1191-2016, 2016.

Gagliardini, O. and Meyssonnier, J.: Flow simulation of a firn-covered cold glacier, Annals of Glaciology, 24, 242–248, 1997.

Gagliardini, O., Zwinger, T., Gillet-Chaulet, F., Durand, G., Favier, L., De Fleurian, B., Greve, R., Malinen, M., Martín, C., and Råback, P.: Capabilities and performance of Elmer/Ice, a new-generation ice sheet model, Geoscientific Model Development, 6, 1299–1318, https://doi.org/10.5194/gmd-6-1299-2013, 2013.

Gilbert, A. and Vincent, C.: Atmospheric temperature changes over the 20th century at very high elevations in the European Alps from englacial temperatures, Geophysical Research Letters, 40, 2102–2108, https://doi.org/10.1002/grl.50401, 2013.

Gilbert, A., Vincent, C., Wagnon, P., Thibert, E., and Rabatel, A.: The influence of snow cover thickness on the thermal regime of Tête Rousse Glacier (Mont Blanc range, 3200 m asl): Consequences for outburst flood hazards and glacier response to climate change, Journal of Geophysical Research, 117, https://doi.org/10.1029/2011JF002258, 2012.

Gilbert, A., Gagliardini, O., Vincent, C., and Wagnon, P.: A 3-D thermal regime model suitable for cold accumulation zones of polythermal mountain glaciers, Journal of Geophysical Research, 119, 1876–1893, https://doi.org/10.1002/2014JF003199, 2014a.

Gilbert, A., Vincent, C., Six, D., Wagnon, P., Piard, L., and Ginot, P.: Modeling near-surface firn temperature in a cold accumulation zone (Col du Dôme, French Alps): from a physical to a semi-parameterized approach, The Cryosphere, 8, 689–703, https://doi.org/10.5194/tc-8-689-2014, 2014b.

https://doi.org/10.5194/egusphere-2026-4058
Preprint. Discussion started: 20 August 2026

Gilbert, A., Vincent, C., Gagliardini, O., Krug, J., and Berthier, E.: Assessment of thermal change in cold avalanching glaciers in relation to climate warming, Geophysical Research Letters, 42, 6382–6390, https://doi.org/10.1002/2015GL064838, 2015.

Gilbert, A., Sinisalo, A., Gurung, T. R., Fujita, K., Maharjan, S. B., Sherpa, T. C., and Fukuda, T.: The influence of water percolation through crevasses on the thermal regime of a Himalayan mountain glacier, The Cryosphere, 14, 1273–1288, https://doi.org/https://doi.org/10.5194/tc-14-1273-2020, 2020.

Gilbert, A., Gimbert, F., Gagliardini, O., and Vincent, C.: Inferring the Basal Friction Law From Long Term Changes of Glacier Length, Thickness and Velocity on an Alpine Glacier, Geophysical Research Letters, 50, e2023GL104 503, https://doi.org/10.1029/2023GL104503, 2023.

Hoelzle, M., Darms, G., Lüthi, M. P., and Suter, S.: Evidence of accelerated englacial warming in the Monte Rosa area, Switzerland/Italy, The Cryosphere, 5, 231–243, https://doi.org/10.5194/tc-5-231-2011, 2011.

Jacob, D., Petersen, J., Eggert, B., Alias, A., Christensen, O. B., Bouwer, L. M., Braun, A., Colette, A., Déqué, M., Georgievski, G., Georgopoulou, E., Gobiet, A., Menut, L., Nikulin, G., Haensler, A., Hempelmann, N., Jones, C., Keuler, K., Kovats, S., Kröner, N., Kotlarski, S., Kriegsmann, A., Martin, E., van Meijgaard, E., Moseley, C., Pfeifer, S., Preuschmann, S., Radermacher, C., Radtke, K., Rechid, D., Rounsevell, M., Samuelsson, P., Somot, S., Soussana, J.-F., Teichmann, C., Valentini, R., Vautard, R., Weber, B., and Yiou, P.: EURO-CORDEX: new high-resolution climate change projections for European impact research, Regional Environmental Change, 14, 563–578, https://doi.org/10.1007/s10113-013-0499-2, 2014.

Krug, J., Weiss, J., Gagliardini, O., and Durand, G.: Combining damage and fracture mechanics to model calving, The Cryosphere, 8, 2101–2117, https://doi.org/10.5194/tc-8-2101-2014, 2014.

Licciulli, C., Bohleber, P., Lier, J., Gagliardini, O., Hoelzle, M., and Eisen, O.: A full Stokes ice-flow model to assist the interpretation of millennial-scale ice cores at the high-Alpine drilling site Colle Gnifetti, Swiss/Italian Alps, Journal of Glaciology, 66, 35–48, https://doi.org/10.1017/jog.2019.82, 2020.

Lüthi, M. P. and Funk, M.: Modelling heat flow in a cold, high-altitude glacier: interpretation of measurements from Colle Gnifetti, Swiss Alps, Journal of Glaciology, 47, 314–324, https://doi.org/10.3189/172756501781832223, 2001.

Margreth, S., Faillettaz, J., Funk, M., Vagliasindi, M., Diotri, F., and Broccolato, M.: Safety concept for hazards caused by ice avalanches from the Whymper hanging glacier in the Mont Blanc Massif, Cold Regions Science and Technology, 69, 194–201, https://doi.org/10.1016/j.coldregions.2011.03.006, 2011.

Maréchal, J. C., Perrochet, P., and Tacher, L.: Long-term simulations of thermal and hydraulic characteristics in a mountain massif: The Mont Blanc case study, French and Italian Alps, Hydrogeology Journal, 7, 341–354, https://doi.org/10.1007/s100400050207, 1999.

Mattea, E., Machguth, H., Kronenberg, M., van Pelt, W., Bassi, M., and Hoelzle, M.: Firn changes at Colle Gnifetti revealed with a high-resolution process-based physical model approach, The Cryosphere, 15, 3181–3205, https://doi.org/10.5194/tc-15-3181-2021, 2021.

Mosbeux, C., Råback, P., Gilbert, A., Brondex, J., Gillet-Chaulet, F., Jourdain, N. C., Chekki, M., Gagliardini, O., and Durand, G.: Development of a Semi-Lagrangian advection scheme in the Finite Element Model Elmer (v9.0): Application to Ice dynamics, EGUsphere, pp. 1–26, https://doi.org/10.5194/egusphere-2025-3039, 2025.

Noetzli, J., Gruber, S., Kohl, T., Salzmann, N., and Haeberli, W.: Three-dimensional distribution and evolution of permafrost temperatures in idealized high-mountain topography, Journal of Geophysical Research: Earth Surface, 112, https://doi.org/10.1029/2006JF000545, 2007.

Oerlemans, J.: Glaciers and climate change, CRC Press, 2001.

https://doi.org/10.5194/egusphere-2026-4058
Preprint. Discussion started: 20 August 2026

Perret, P., Fosson, J. P., Mondardini, L., Segor, V., Perret, P., Fosson, J. P., Mondardini, L., and Segor, V.: Val Ferret Pilot Action Region: Grandes Jorasses Glaciers - An Open-Air Laboratory for the Development of Close-Range Remote Sensing Monitoring Systems, IntechOpen, ISBN 978-1-83969-329-8, https://doi.org/10.5772/intechopen.99013, 2021.

Phillips, T., Rajaram, H., and Steffen, K.: Cryo-hydrologic warming: A potential mechanism for rapid thermal response of ice sheets, Geophysical Research Letters, 37, https://doi.org/10.1029/2010GL044397, 2010.

Pralong, A. and Funk, M.: On the instability of avalanching glaciers, Journal of Glaciology, 52, 31–48, https://doi.org/10.3189/172756506781828980, 2006.

Sauter, T., Arndt, A., and Schneider, C.: COSIPY v1.3 – an open-source coupled snowpack and ice surface energy and mass balance model, Geoscientific Model Development, 13, 5645–5662, https://doi.org/10.5194/gmd-13-5645-2020, 2020.

Verjans, V., Leeson, A. A., Stevens, C. M., MacFerrin, M., Noël, B., and van den Broeke, M. R.: Development of physically based liquid water schemes for Greenland firn-densification models, The Cryosphere, 13, 1819–1842, https://doi.org/10.5194/tc-13-1819-2019, 2019.

Vernay, M., Lafaysse, M., Monteiro, D., Hagenmuller, P., Nheili, R., Samacoïts, R., Verfaillie, D., and Morin, S.: The S2M meteorological and snow cover reanalysis over the French mountainous areas, description and evaluation (1958–2020), Earth System Science Data Discussions, pp. 1–36, https://doi.org/10.5194/essd-2021-249, 2021.

Vincent, C., Le Meur, E., Six, D., Funk, M., Hoelzle, M., and Preunkert, S.: Very high-elevation Mont Blanc glaciated areas not affected by the 20th century climate change, Journal of Geophysical Research: Atmospheres, 112, D09 120, https://doi.org/10.1029/2006JD007407, 2007a.

Vincent, C., Le Meur, E., Six, D., Possenti, P., Lefebvre, E., and Funk, M.: Climate warming revealed by englacial temperatures at Col du Dôme (4250 m, Mont Blanc area), Geophysical Research Letters, 34, L16 502, https://doi.org/10.1029/2007GL029933, 2007b.

Vincent, C., Gilbert, A., Jourdain, B., Piard, L., Ginot, P., Mikhalenko, V., Possenti, P., Meur, E. L., Laarman, O., and Six, D.: Strong changes in englacial temperatures despite insignificant changes in ice thickness at Dôme du Goûter glacier (Mont Blanc area), The Cryosphere, 14, 925–934, https://doi.org/https://doi.org/10.5194/tc-14-925-2020, 2020.

Vionnet, V., Brun, E., Morin, S., Boone, A., Faroux, S., Le Moigne, P., Martin, E., and Willemet, J.-M.: The detailed snowpack scheme Crocus and its implementation in SURFEX v7.2, Geosci. Model Dev., 5, 773–791, https://doi.org/10.5194/gmd-5-773-2012, 2012.

Zwinger, T., Greve, R., Gagliardini, O., Shiraiwa, T., and Lyly, M.: A full Stokes-flow thermo-mechanical model for firn and ice applied to the Gorshkov crater glacier, Kamchatka, Annals of Glaciology, 45, 29–37, https://doi.org/10.3189/172756407782282543, 2007.